Available online at www.sciencedirect.com

jmr&t Journal of Materials Research and Technology

www.jmrt.com.br

Original Article

Self-healing capability of asphalt concrete with carbon-based materials

Doo-Yeol Yoo [a], Soonho Kim [a,*], Min-Jae Kim [a], Doyeong Kim [a], Hyun-Oh Shin [b,**]

[a] Department of Architectural Engineering, Hanyang University, 222 Wangsimni-ro, Seongdong-gu, Seoul 04763, Republic of Korea
[b] Department of Agricultural and Rural Engineering, Chungnam National University, 99 Daehak-ro, Yuseong-gu, Daejeon 34134, Republic of Korea

ARTICLE INFO

Article history:
Received 5 March 2018
Accepted 2 July 2018
Available online 1 August 2018

Keywords:
Asphalt concrete
Carbon materials
Mechanical property
Self-healing capability
Induction heating

ABSTRACT

This study aims to investigate the effect of carbon-based materials, i.e., carbon fibers (CFs), carbon nanotubes (CNTs), and graphite nanofibers (GNFs), on the mechanical and self-healing properties of asphalt concrete. For this, 0.5% CF, CNT, and GNF, and 1.0% CF were incorporated, and plain asphalt concrete was also considered for comparison. The self-healing capability of asphalt concrete was examined based on induction heating and was quantitatively evaluated by comparing the flexural strengths of virgin and healed specimens. Test results indicated that adding the carbon nanomaterials, i.e., CNTs and GNFs, was more effective in improving the Marshall stability, indirect tensile strength, and dynamic stability, and reducing the porosity, compared to adding macro CFs. However, the flexural performance of asphalt concrete was more efficiently enhanced by adding the CFs relative to CNTs and GNFs. Asphalt concrete specimens that completely failed under flexure were partially self-healed using induction heating due to the incorporated carbon materials. The best healing capability, i.e., 40% recovery of the original flexural strength, was obtained for the specimens with 0.5% GNFs and CFs.

1. Introduction

For a very long time, asphalt concrete has been the most frequently used material for pavements of highways and roads. More than 90% of roads are surfaced with asphalt concrete in USA, and a great part of roads in other countries are also fabricated with asphalt concrete. Most countries have adopted asphalt concrete for highways and roads because it is economical, durable, safe, and recyclable. Roads are quickly and economically built using asphalt concrete, which minimizes traffic problems and economic loss. Asphalt concrete pavement can also lead to improvements in ride quality compared to concrete pavement, and it is largely recycled by the asphalt industry. However, since asphalt concrete is a type of flexible

* *Corresponding author*. Tel.: +82 2 2220 2373.
** *Corresponding author*. Tel.: +82 42 821 5798.
E-mails: tnsgh0905@hanyang.ac.kr (S. Kim), hyunoh.shin@cnu.ac.kr (H. Shin).

https://doi.org/10.1016/j.jmrt.2018.07.001

pavement, some drawbacks such as plastic deformation, potholes, and settlement are also observed, and these deteriorate the service life and performance of asphalt concrete. Therefore, numerous previous studies [1–9] have been performed to improve the performance of asphalt concrete by including various types of reinforcements, i.e., steel and synthetic fibers, and nanomaterials.

Abtahi et al. [2] have reviewed the performances of asphalt concrete including various types of fibers. Based on their [2] examination, adding fibers as a reinforcement to asphalt concrete improved the dynamic modulus, moisture susceptibility, creep compliance, rutting resistance, and freeze-thaw resistance. Park et al. [5] conducted indirect tensile tests at low temperature (−20 °C) to evaluate the effects of steel, carbon, and polyvinyl alcohol (PVA) fibers on the cracking resistance of asphalt concrete. Several important findings were reported, as follows: (1) longer, smooth steel fibers effectively improve the indirect tensile strength and toughness relative to shorter ones, (2) deformed steel fibers, i.e., hooked and twisted fibers, improved toughness but did not provide any benefits in terms of the strength compared to smooth fibers, and (3) using the steel fibers enhances toughness of asphalt concrete more than using the carbon and PVA fibers. Tapkın [6] examined the effect of polypropylene (PP) fibers on the performance of asphalt concrete and reported that the use of PP fibers is beneficial for improving Marshall stability, fatigue life, rutting resistance, and resistance to reflection cracking. The effects of nylon and cellulose fibers on the performance of asphalt concrete have also been evaluated by Lee et al. [7], Selim et al. [8], and Wu et al. [9]. An asphalt concrete mixture with 1% (by volume) 12-mm nylon fibers exhibited 85% greater fracture energy absorption capacity than plain asphalt mixture without fibers, leading to enhanced resistance to fatigue cracks [7]. Also, higher dynamic modulus and indirect tensile strength were obtained for asphalt concrete with cellulose fibers as compared with those of plain asphalt concrete [8,9]. Yang et al. [10] used a new type of fiber, called amorphous metallic fiber, in an asphalt concrete mixture and examined various mechanical properties. Their experimental results [10] showed that the dynamic stability, strain capacity, and thermal conductivity of asphalt concrete could be improved by incorporating 0.5–1.5% (by volume) amorphous fibers, whereas the indirect tensile strength and flexural strength were reduced. Approximately 6% asphalt binder is needed to achieve a porosity of 4% or less for amorphous fiber-reinforced asphalt concrete, which was higher than that (4.8%) of plain asphalt concrete. Latifi and Hayati [4] have developed hot mix asphalt including carbon nanotubes (CNTs) that show improved rutting resistance, stiffness, and fatigue performance (especially at low temperature) compared to plain asphalt. They [4] suggested an optimum weight percentage of CNTs in the hot mix asphalt of 1%. Faramarzi et al. [1] reported that the addition of CNTs resulted in an enhancement in the Marshall stability of asphalt concrete.

Liu et al. [11] developed conductive asphalt concrete using short steel fibers and long steel wool. Based on their test results, 10% (by volume of bitumen) steel wool was suggested for making a conductive asphalt concrete with acceptable indirect tensile strength by fast induction heating. The temperature of asphalt concrete by induction heat was significantly increased by increasing the steel wool volume content up to 10%, and it reached almost 140 °C at only 180 s. Liu et al. [12] also verified that the application of induction heating enhanced the fatigue life extension ratio, $\Delta f/f$, of steel wool reinforced porous and conductive asphalt concrete. Here, Δf is the extra fatigue life after damage, and f is the original fatigue life. An optimum heating temperature of 85 °C was suggested to obtain the best healing effect. García et al. [13] adopted steel wool for fabricating conductive asphalt concrete, similar to previous studies [11,12], but they used it in dense asphalt concrete mixtures. They successfully developed a conductive asphalt concrete with steel wool showing a maximum temperature of 90 °C after 1 min of induction heating. They recommended using short fibers with large diameters for induction heating. Yang et al. [10] adopted a newly developed amorphous metallic fiber to fabricate conductive asphalt concrete. The maximum internal temperature of 72.3 °C was achieved by adding 3% amorphous fibers into the asphalt mixture, and the completely broken specimen was well adhered by the induction heating process. Wang et al. [14] examined the microwave healing of carbon fiber reinforced asphalt concrete under several cycles of fracture and verified a partial recovery of cracked asphalt concrete with carbon fibers by a microwave healing process. Ajam et al. [15] also compared two different approaches, i.e., induction heating and infrared radiation, for healing conductive asphalt concrete with a metal grit. They showed that the induction heating method requires much shorter times and less energy for self-healing than infrared radiation.

The induction heating method can be effective for in situ application of healing cracks in asphalt concrete. Once pothole or severe cracks are formed in asphalt pavement, a movable induction heating machine can be used to melt down bitumen in asphalt concrete, and the melted asphalt concrete can then be compacted by using roller. Based on this simple repairing process, the amount of asphalt waste is able to be reduced and we can achieve sustainable development in terms of road engineering.

Numerous studies have been conducted to improve the mechanical properties and durability of asphalt concrete and to achieve its self-healing capability as mentioned above. However, to the best of the authors' knowledge, there is no published paper examining the effect of carbon materials on both the mechanical and self-healing properties of asphalt concrete to determine the optimum type of carbon material. Thus, in this study, the effectiveness of using three different types of carbon-based materials, i.e., carbon fiber (CF), CNT, and graphite nanofiber (GNF), on improving the various mechanical properties of asphalt concrete was evaluated. Using the induction heating method, the self-healing capabilities of completely broken asphalt concrete specimens with and without carbon materials were also examined under a restrained condition, and their self-healing capability was quantitatively estimated.

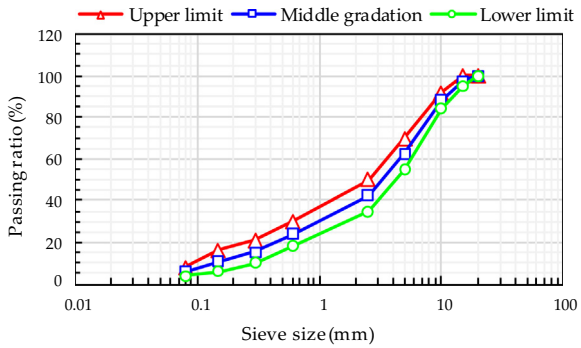

Fig. 1 – Passing ratio versus particle size curves of aggregates.

2. Experimental program

2.1. *Materials and mixing sequence*

WC-2 type aggregate was adopted to fabricate ordinary asphalt concrete frequently used in South Korea. This material is normally applied to a surface layer of asphalt pavement. The detailed requirements of WC-2 type of aggregate are given in a guideline [16], and it is produced by mixing 13-mm aggregate, crushed sand, and filler. This aggregate type can provide a more compacted macrostructure of asphalt concrete than other types of aggregate. The passing ratio (%) and particle size (mm) curves of the used WC-2 type of aggregate are shown in Fig. 1. Before mixing the aggregates with bitumen, they were dried in a desiccator with a temperature of 110 °C until there was no change in weight per unit volume. The asphalt content used was 5.34%, and all tested samples were fabricated using the same asphalt concrete mixture. The aggregate was then mixed with bitumen, and the viscosity was maintained to be 170 ± 20 and 280 ± 30 centistoke (cSt) during the mixing and compaction processes, respectively. In order to fabricate compact asphalt concrete samples, they were compacted 75 times using a compaction machine in Fig. 2. After that, asphalt concrete mixture was cured in an oven with a high temperature of 135 °C.

We added several types of carbon-based materials (i.e., CF, CNT, and GNF) into the mixture to enhance the mechanical properties and achieve self-healing capacity in asphalt concrete. The geometrical and physical properties of the used carbon materials are given in Table 1 and their scanning electron microscope (SEM) images can be found elsewhere [17,18]. In order to improve uniform dispersion of the carbon-based materials, the asphalt concrete mixture was mixed additionally for 10 min after adding the carbon-based materials, CF, CNT, and GNF. The melting point of all the materials was over 1000 °C, meaning that there was no melting of carbon materials during mixing process. In addition, extremely high tensile strengths were obtained for the CF, CNT, and GNF, such as 4,900 MPa, over 11,000 MPa, and over 1,860 MPa, respectively. Therefore, we did not expect breakage of the carbon materials during the pulling out process. The size of the CF was much greater than those of GNF and CNT, but they had a similar aspect ratio (l_f/d_f), ranging from 50 to 2000. Herein, l_f is the fiber length and d_f is the fiber diameter. The length of CF was about 1200 times larger than those of CNT and GNF. Although the lengths of CNT and GNF were quite similar, the diameter of CNT was about 10 times smaller than that of GNF, meaning that much higher number of CNTs was incorporated into the mixture than the counterpart. The highest density of 1.94 g/cm^3 was obtained in the GNF, while similar densities were found for the CF and CNT. A multi-walled CNT was adopted instead of a single-walled CNT, because the former is less expensive and has a higher tensile strength [19,20] than the latter, leading to better reinforcement in asphalt concrete. Two different volume fractions (i.e., 0.5% and 1.0%) were applied for the case of CF, while a single volume fraction, 0.5%, was adopted for the cases of CNT and GNF. Lee et al. [17] recently reported that using CNTs is more effective in improving conductivity of cement composites than using CFs at identical volume fractions. Thus, the higher volume fraction of 1.0% was only applied for the CF. It must be noted that the prices of CNT and GNF are much expensive than CF and all other ingredients included in the asphalt concrete mixture. The successful development of self-healing asphalt concrete products using the carbon materials gives a benefit for sustainable development of road engineering by reducing the amount of asphalt waste, but for their practical application, the cost effectiveness needs to be solved at the same time.

The notation of the test variables contains carbon material type and volume fraction. The words 'CF,' 'CNT,' and 'GNF' denote carbon materials, and the following numeral indicates volume fraction. For instance, an asphalt concrete reinforced with 1.0% CFs is denoted as CF1.0. As a control specimen, plain asphalt concrete, denoted as 'Plain,' was also used in this study.

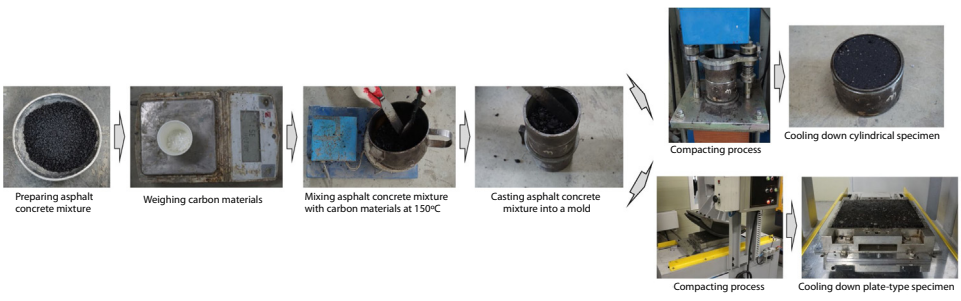

Fig. 2 – Preparation of asphalt concrete specimens.

Table 1 – Geometrical and physical properties of carbon-based materials.

	CF	CNT	GNF
Density (g/cm^3)	1.37	1.30	1.94
Elastic modulus (GPa)	230	–	–
Melting point (°C)	Over 1000	Over 1000	Over 1000
Tensile strength (MPa)	4900	Over 11,000	Over 1860
Length, l_f (μm)	12,000	10	10–30
Diameter, d_f (nm)	7000	5–20	50–200
Feature	Single chopped	Multi–walled	–

Note: CF = carbon fiber, CNT = carbon nanotube, and GNF = graphite nanofiber.

2.2. *Specimen preparation*

To evaluate the effect of carbon materials on the mechanical properties and durability of asphalt concrete, five different tests in terms of, (1) Marshall stability, (2) porosity, (3) indirect tensile strength, (4) dynamic stability, and (5) flexural performance, were performed. In addition, to obtain reliable test results, two or three samples were fabricated and tested for each variable and average values were adopted. Cylindrical specimens were fabricated and used for tests from 1 to 3, while plate specimens were adopted for the last two tests (i.e., 4 and 5). Once the asphalt concrete mixing process was completed, the material was cast into a cylindrical mold with a diameter of 101.6 mm and a height of 76.2 mm. Then, they were compacted 75 times using a hammer with a weight of 4.5 kg dropped at a height of 450 mm for both sides. The rate of hammer compacting was 60 times per min. The detailed process of specimen preparation is shown in Fig. 2. Cylindrical specimens with a diameter of 101.6 mm and a height of 63.5 mm were finally fabricated based on this manufacturing process, and they were cured in a laboratory at room temperature to be gradually cooled down to ambient temperature.

A square plate-type mold with a width of 300 mm and a height of 50 mm was used to fabricate wheel tracking test specimens for dynamic stability. Once the asphalt concrete mixture was cast into the mold, they were also compacted using a roller compacter with a maximum compacting load of 8.82 kN to have a density similar to the cylindrical specimen. To effectively compact the specimen, the temperatures of the mold and roller were maintained to be about 140 °C. The $300 \times 300 \times 50$ mm^3-sized plate-type specimen was also used for evaluating the flexural performance by cutting it into three equal pieces with a width of 100 mm. Thus, the manufacturing processes of the wheel tracking and flexural specimens were identical, but the sizes were only different.

2.3. *Test setups*

2.3.1. *Marshall stability and flow test*

The Marshall stability test was carried out according to ASTM D1559 [21] to evaluate the compressive strength and deformability of asphalt concrete. Before applying a uniaxial load, the cylindrical specimen was immersed into a water tank for 30 min to reach a high material temperature of 60 °C. The temperature of the loading head was also high as 40 °C. Since the stability of asphalt concrete was measured at such a high temperature, our evaluations of stability are conservative because lower viscosity and adhesion of bitumen were obtained at high temperature [22]. A universal testing machine (UTM) with a maximum loading capacity of 25 kN was used for applying a uniaxial load as shown in Fig. 3a. A cylindrical specimen with a diameter of 101.6 mm and a height of 63.5 mm was placed under the semicircular loading head to provide a uniform compressive load, as shown in Fig. 3b. The load was applied through displacement control with a rate of 50.8 mm/min, and this Marshall stability test was completed within 30 s from taking the samples from the water tank as per ASTM D1559 [21]. The terms, Marshall stability and flow, indicate the maximum compressive load and the corresponding deformation, respectively. Three specimens were used for each test variable to obtain reliable average values of Marshall stability and flow.

2.3.2. *Test for air void content*

To evaluate the porosity of asphalt concretes with and without carbon-based materials, the air void content was calculated by measuring the density of the cylindrical specimen. For this, three cylindrical specimens identical to those used for the Marshall stability measurement were used for each variable to obtain an average value. To calculate the porosity, we first measured the bulk density of the specimen in accordance with KS F 2364 [23]. The density of the asphalt concrete mixture without voids was calculated theoretically based on the exact percentage of materials and their densities, which were given by manufacturers.

2.3.3. *Indirect tensile strength test*

The tensile strengths of all asphalt concrete mixtures were measured by performing an indirect tensile strength test according to ASTM D 6931 [24]. The uniaxial compressive load was also applied using the UTM used for the Marshall stability measurement (Fig. 3a), but the loading head was flat to provide tensile stress in the specimen, similar to the Brazilian test. The picture of the test setup is given in Fig. 3c. Other testing conditions were exactly identical with those of the Marshall stability test, i.e., high temperatures (40 and 60 °C), loading rate (50.8 mm/min), and operating time (30 s).

2.3.4. *Wheel tracking test (dynamic stability)*

The dynamic stability of asphalt concrete is the most important factor affecting plastic deformation of road pavement. Thus, it was evaluated by performing a wheel tracking test according to KS F 2374 [25], and the detailed test setup is shown in Fig. 4. For this, we have used a plate-type specimen with a dimension of $300 \times 300 \times 50$ mm^3, and its resistance

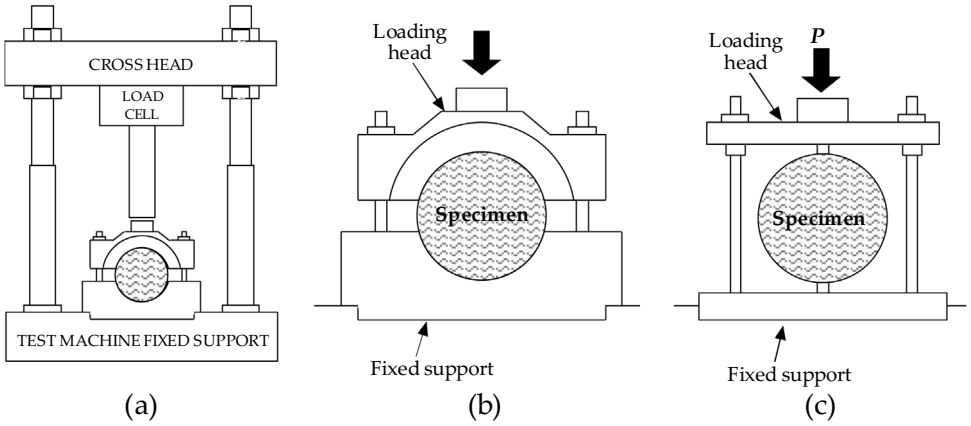

Fig. 3 – Test setup for Marshall stability and indirect tensile strength.

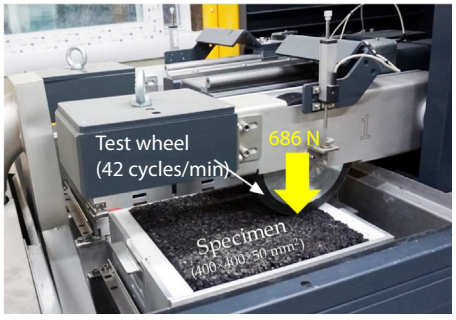

Fig. 4 – Test setup for wheel tracking test.

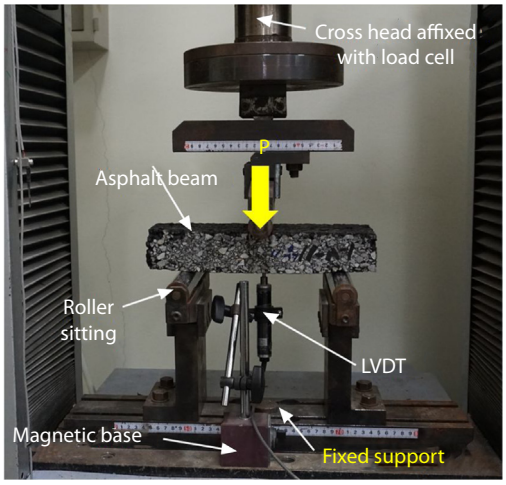

Fig. 5 – Three-point bending test setup.

to the dynamic wheel force was measured at a high temperature. The test specimen and inside of the test apparatus were maintained to have a high temperature of about 60 °C to conservatively evaluate dynamic stability like the previous Marshall stability test. The diameter and width of the wheel used for the dynamic stability measurement were 200 mm and 50 mm, respectively, and the rubber thickness was 15 mm. The tracking wheel was moved back and forth repeatedly with a vertical pressure of 686 N applied to the asphalt concrete specimen, and the speed of the wheel was 42 cycles per min. The dynamic stability of asphalt concrete was evaluated based on the number of wheel movements resulting in 1 mm deformation.

2.3.5. *Three-point bending test*

The flexural strength and strain capacity of asphalt concrete were evaluated by performing a three-point bending test as per KS F 2395 [26]. KS F 2395 [26] states that the flexural strength and strain capacity need to be measured at a low temperature of −10 °C. However, since we normally use the asphalt concrete at ambient temperature, the bending tests were carried out at both ambient and low temperatures. To measure the flexural performance, the fabricated plate-type specimen was cut into three pieces to dimensions of $300 \times 100 \times 50\,mm^3$. A uniaxial load was applied through a UTM with a maximum loading capacity of 250 kN under displacement control. The clear span length was 200 mm, and the mid-span deflection (required for calculating the strain) was measured using a linear variable differential transformer (LVDT) and stroke at the ambient and low temperature conditions, respectively. The test setup for the three-point bending test of asphalt concrete at ambient temperature is shown in Fig. 5.

2.3.6. *Induction heating test*

To investigate the effect of carbon materials, i.e., CF, CNT, and GNF, on the self-healing capability of the damaged asphalt concrete, the completely destroyed three-point bending specimens were used for the induction heating test. Induction heating was applied for damaged asphalt concrete specimens using a heat generator with a capacity of 30 kW at a frequency of 88 kHz for 20 min. Single crack near the center of the specimens was obtained. For healing the crack formed, the center of broken asphalt concrete specimens was locally enclosed with induction heating coil, and then, the induction heating was applied. To evaluate the temperature variation of asphalt concrete during the induction heating process, an infrared thermographic camera was used, and its temperature variation was recorded. The picture of the induction heating test setup is given in Fig. 6. Immediately

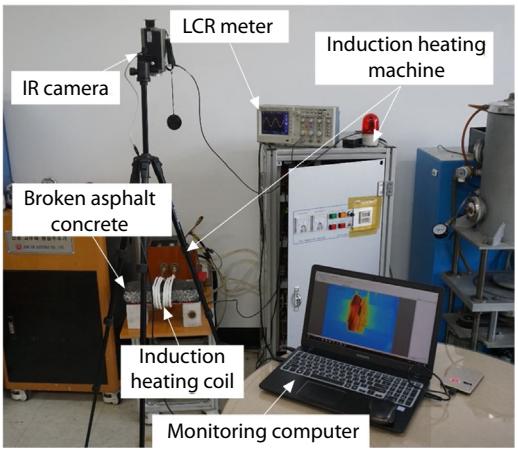

Fig. 6 – Picture for induction heating test setup.

after finishing the induction heating process, the specimens were restrained by using a special containment device and cured at room temperature to gradually reduce their inner temperature to ambient temperature for 24 h.

2.4. *Test parameters*

The various parameters for the performance evaluation of asphalt concrete are summarized as follows. First, the porosity, which is the void volume fraction among the total volume of asphalt concrete, was calculated based on the following equation, given by KS F 2364 [23]:

$$P = \left(1 - \frac{D_p}{D_t}\right) \times 100 \tag{1}$$

where P is the porosity (%), D_b is the bulk specific gravity, and D_t is the maximum theoretical specific gravity. The bulk specific gravity and the maximum theoretical specific gravity were given by KS F 2446 [27] and KS F 2366 [28], respectively.

Indirect tensile strengths of the asphalt concrete can be calculated as follows:

$$S_r = \frac{2P}{\pi D h} \tag{2}$$

where S_T is the indirect tensile strength, P is the maximum load, D is the diameter of the cylinder, and h is the height of the cylinder.

The dynamic stability under repeated wheel tracking can be calculated based on a concept used to calculate the total number of horizontal movements of the wheel required per 1-mm deformation, as follows

$$DS = N \times \frac{t_2 - t_1}{d_2 - d_1} \tag{3}$$

Here, DS is the dynamic stability, N is the speed of the wheel (42 cycles per min), d_1 and d_2 are the displacements of specimens measured at t_1 and t_2, respectively, and t_1 and t_2 are typically 45 and 60 min, respectively.

A rate of deformation of the specimen (in mm/min) under repeated wheel movements is also calculated as follows:

$$RD = \frac{d_{60} - d_{45}}{15} \tag{4}$$

where RD is the rate of deformation, and d_{45} and d_{60} are the amounts of deformation measured at 45 and 60 min, respectively.

The flexural stress and strain under three-point bending load are calculated as follows:

$$\sigma = \frac{3Pl}{2bh^2} \tag{5}$$

$$\varepsilon = \frac{6hd}{l^2} \tag{6}$$

where σ is the flexural stress, ε is the flexural strain, P is the applied load, l is the clear span length, b is the beam width, h is the beam height, and d is the mid-span deflection.

3. Experimental results and discussion

3.1. *Marshall stability and flow*

The Marshall stability and flow values of asphalt concretes with and without carbon materials are given in Fig. 7. The Marshall stability of asphalt concrete was noticeably enhanced by including carbon nanomaterials, such as CNT and GNF, whereas it was insignificantly changed by the existence and volume fraction of CF. For instance, the Marshall stabilities of CNT0.5 and GNF0.5 were found to be 13.9 and 14.2 kN, respectively, which are approximately 25% and 28% higher than that of plain asphalt concrete. In the same vein, the CNT0.5 and GNF0.5 specimens exhibited lower flow values as compared to the plain specimen, meaning that they effectively limited the deformation under compressive force. However, the specimens with CFs showed similar flow values with that of the plain specimen. The sizes of CNT and GNF were very small (on the nanometer scale) as given in Table 1, so that they might effectively fill the pores inside the mixture even at such a small dosage. In the same vein, Faramarzi et al. [29] have also reported the improved mechanical properties of asphalt concrete by including only small amount of CNTs. The improvement in Marshall stability of asphalt concrete by adding CNT and GNF was thus caused by the filling effects of the pores, leading to a denser microstructure. The enhanced Marshall stability of the asphalt concrete mixture by adding CNTs was also reported by Ziari et al. [30] and Faramarzi et al. [1]. In their study [1,30], the Marshall stability of asphalt concrete increased with increasing the amount of CNTs, and approximately 15% and 39% higher stability was obtained by adding 0.5% and 0.6% (by weight) CNTs, respectively. Although adding both the CNT and GNF improved the Marshall stability of asphalt concrete, the latter gave slightly better results than the former. The insignificant change in Marshall stability of the specimens with CFs was caused by insufficient dispersion of the fibers, as shown in Fig. 8. In order to evaluate the dispersion of carbon-based materials, SEM images on the crack surface of asphalt concrete beams were taken

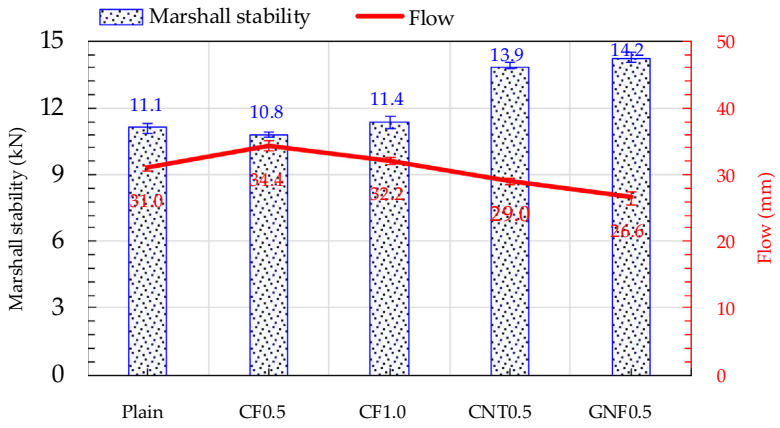

Fig. 7 – Effect of carbon materials on Marshall stability of asphalt concrete.

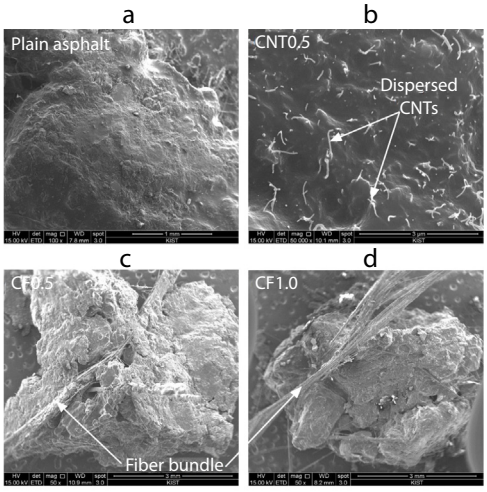

Fig. 8 – SEM images of (a) plain asphalt concrete, (b) asphalt concrete with 0.5% CNTs, (c) asphalt concrete with 0.5% CFs, and (d) asphalt concrete with 1.0% CFs.

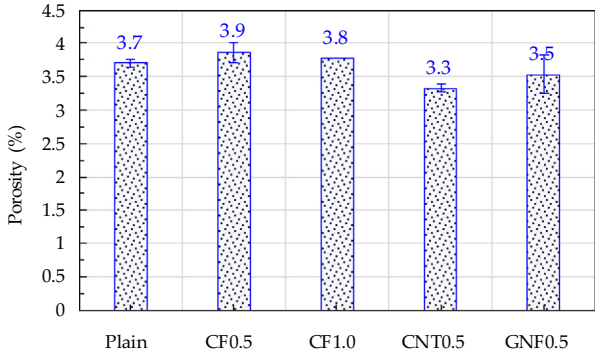

Fig. 9 – Effect of carbon materials on air void content of asphalt concrete.

after finishing the bending tests. Since the bending test specimens were fabricated by cutting the plate-type specimen for the Marshall stability specimens, similar degree of dispersion of carbon materials was assumed to be obtained. As compared to the case of CNTs in Fig. 8b, the degree of dispersion of CFs was very poor. Since the CNT has much higher aspect ratio than that of GNF (Table 1), it was expected that the uniform dispersion of CNT is much difficult to be obtained than the latter, so that only the SEM images of CNT and CF were compared. Obtaining good dispersion of the CFs was difficult during the mixing process because they were shipped in bundles and had very high aspect ratio (l_f/d_f) over 1000. This could be verified by SEM images in Fig. 8, indicating that the bundled CFs were observed in the asphalt concrete mixture. The difficulties of mixing for carbon fiber reinforced asphalt concrete also have been reported by Park et al. [5], limiting the improvement of the post-cracking ductility. For these reasons, a minor change or even slight decrease of Marshall stability of asphalt concrete by including carbon fibers was similarly observed in a previous study performed by Khabiri and Alidadi [3].

3.2. *Air void content*

Fig. 9 shows the comparative porosity of asphalt concrete with and without various carbon materials. The amount of air voids, represented by the porosity in Fig. 9, was slightly increased by including CFs, whereas it decreased by adding CNTs and GNFs. The increased air void contents in the asphalt concrete by adding the CFs was also reported by Abtahi et al. [2]. This is because the bundled CFs formed fiber balls and were not dispersed well (Fig. 8). Thus, they disturbed the asphalt concrete mixture to be effectively compacted, resulting in an increase in pores. On the other hand, the amount of air voids inside the asphalt mixture was reduced by the carbon nanomaterials, i.e., CNT and GNF, because they filled the pores. As shown in Fig. 8b, the CNT was well dispersed in the asphalt mixture in a qualitative sense, and the sizes of CNT and GNF were much smaller than the aggregates. Thus, the various-sized pores formed in the asphalt concrete could be filled by the CNTs and GNFs. The CNTs were more effective in the filling capacity of pores in asphalt concrete than the GNFs, due to their smaller size, causing the smallest porosity, as given in Fig. 9.

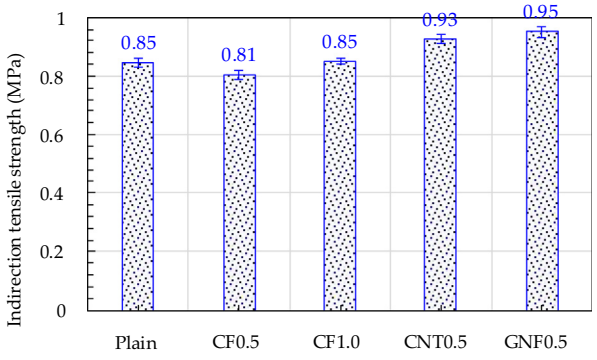

Fig. 10 – Effect of carbon materials on indirect tensile strength of asphalt concrete.

3.3. *Indirect tensile strength*

The effects of CF, CNT, and GNF on the indirect tensile strength of asphalt concrete are shown in Fig. 10. Similar to the previous Marshall stability test results, the additions of 0.5% CNT and GNF were effective in enhancing the indirect tensile strength of plain asphalt concrete, but the 0.5% CFs did not noticeably affect the strength. For instance, an indirect tensile strength of 0.85 MPa was obtained for the plain asphalt concrete, while approximately 10% and 13% higher values were measured for the CNT0.5 and GNF0.5 specimens. However, values similar to or slightly lower than the plain specimen were observed for the CF specimens (i.e., CF0.5 and CF1.0). This is consistent with the findings from Park et al. [5], who reported that the improvement of indirect tensile strength by adding carbon fibers into the asphalt mixture is limited relative to other synthetic and steel fibers because of the mixing difficulties. The asphalt mixing process becomes difficult as the carbon fibers are incorporated due to their very high aspect ratio and tendency to be tangled. Also, Latifi and Hayati [4] similarly reported an increase in the indirect tensile strength of asphalt concrete by adding CNTs and increasing their amount. In their study, the increase rate of the indirect tensile strength was highest at a CNT content of 0.5% for the mixture with dry CNTs. Higher indirect tensile strengths were obtained by adding CNTs and GNFs in this study, because they effectively resisted tensile force at the point where specimen rupture occurred by the bridging effect. Due to their very high tensile strengths (Table 1), they were not ruptured during the pulling out process, so that excellent crack bridging capacity was obtained. Also, since they filled the pores in asphalt concrete, a denser microstructure was achieved, and this caused a higher indirect tensile strength and stiffening of the asphalt concrete.

3.4. *Dynamic stability*

Fig. 11 shows the dynamic stability and rate of deformation for all the tested specimens. The dynamic stability of plain asphalt concrete was only improved by incorporating 0.5% GNFs, while the additions of CF and CNT did not provide any noticeable changes. For example, the highest dynamic stability of GNF0.5 was found to be about 3182 cycles/mm, which was approximately 42% higher than that of plain asphalt concrete. The rate of deformation was insignificantly changed by adding CFs and CNTs but greatly reduced by adding GNFs, as shown in Fig. 11. This means that the inclusion of GNF into the asphalt mixture is effective in delaying the increase in deformation by repeated wheel loads, because the GNF resisted the propagation and widening of cracks formed in the asphalt concrete by the wheel load, limiting the increase in the permanent deformation. The lowest rate of deformation was also obtained for the GNF0.5 specimen, and it was approximately 40% lower than that of the plain asphalt concrete. On the other hand, Amirkhanian et al. [31] and Yang and Tighe [32] reported the enhancement of rutting resistance, represented by the dynamic stability, of asphalt concrete by adding the CNTs, which is inconsistent with the findings of this study.

3.5. *Flexural performance*

Fig. 12 shows the flexural stress versus strain curves of all tested specimens at low (−10 °C) and ambient (20 °C) temperatures. In addition, the flexural strength and strain capacity are all summarized in Fig. 13. Higher flexural strength and stiffness were obtained at low temperature compared to those under the ambient temperature. This is consistent with the findings from Yang et al. [10] and Qiu et al. [33]. Qiu et al. [33] reported that the flexural strength of asphalt concrete increased with a decrease in temperature from 80 °C to −30 °C.

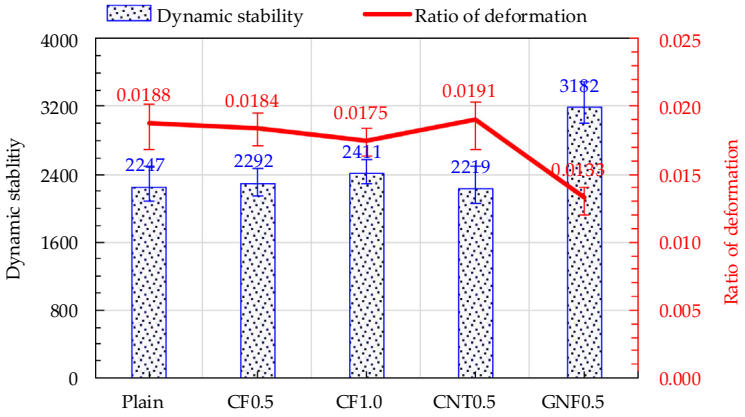

Fig. 11 – Effect of carbon materials on dynamic stability and rate deformation of asphalt concrete.

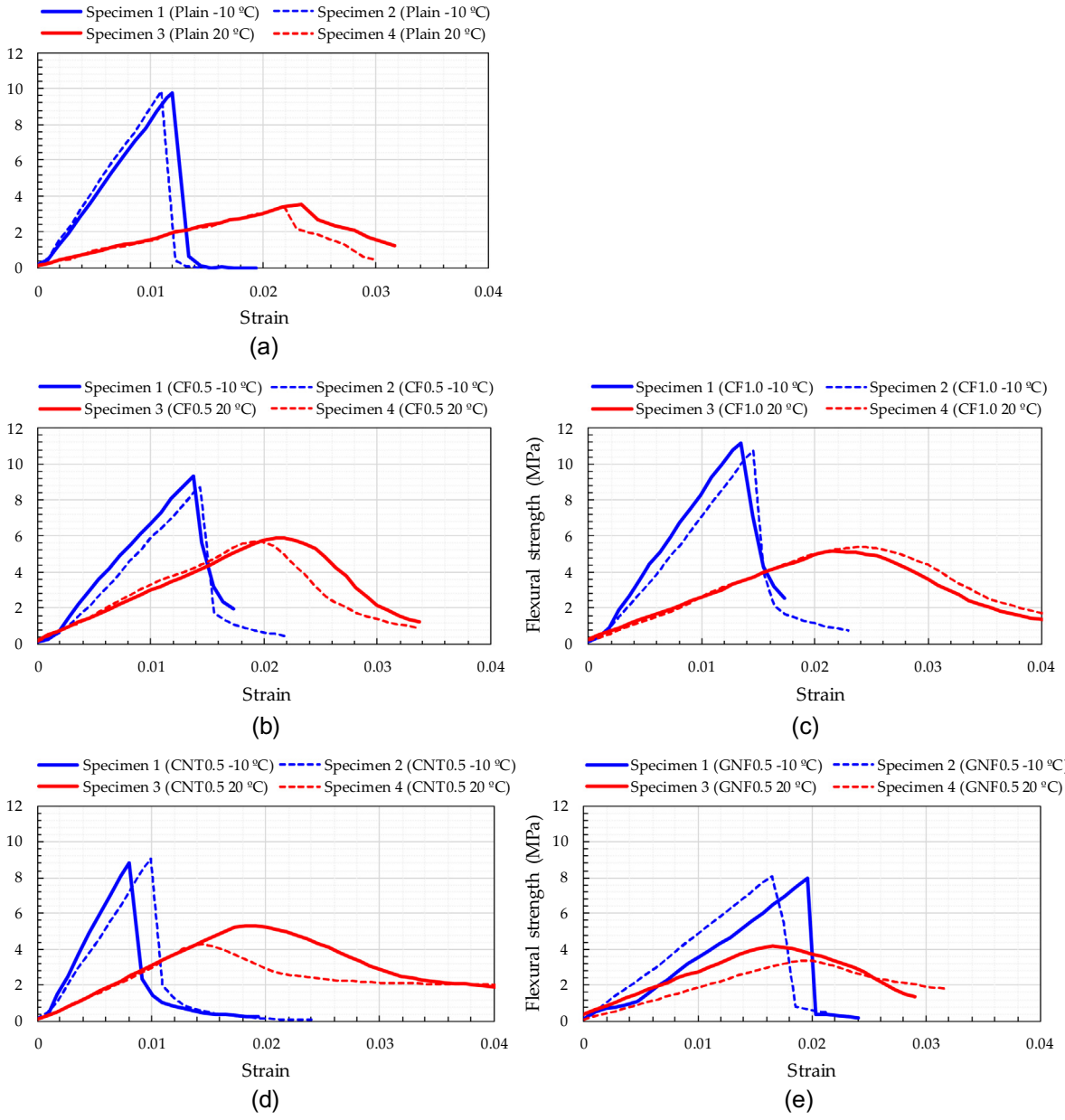

Fig. 12 – Flexural stress versus strain curves for (a) plain asphalt, (b) CF0.5, (c) CF1.0, (d) CNT0.5, and (e) GNF0.5.

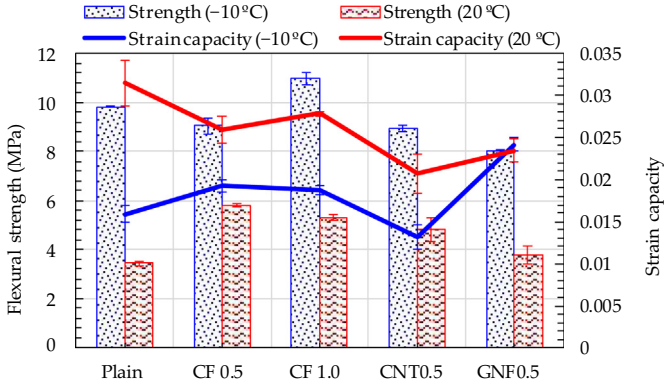

Fig. 13 – Effect of carbon materials on flexural performance of asphalt concrete.

The reason for increasing flexural strength at lower temperature is that the pores are filled with the expanded frozen solution due to freezing of the pore solution at sub-zero temperatures, resulting in a denser microstructure [10]. However, the brittleness of the asphalt concrete specimens under flexure became more obvious at the low temperature than that at ambient temperature. This is also consistent with the test results of Yang et al. [10] for asphalt concrete reinforced with amorphous metallic fibers. As shown in Fig. 13, smaller strain capacities were obtained at a low temperature of −10 °C than those at an ambient temperature of 20 °C, although the former exhibited about 1.6–2.8 times higher flexural strengths than the latter. In addition, a gradual decrease in the post-peak flexural stress with respect to the strain was observed for the specimens at ambient temperature compared to their counterparts.

Most of the asphalt concrete specimens including carbon materials exhibited higher flexural strength than that of the plain specimen at an ambient temperature of 20 °C. Although the GNF0.5 specimen exhibited higher average flexural strength value than the plain asphalt concrete, its increment was relatively marginal than other carbon materials. The flexural strength of plain asphalt concrete was generally reduced by including the carbon materials at low temperature, except for the CF1.0 specimen. This means that the effectiveness of adding carbon nanomaterials, i.e., CNT and GNF, on the flexural strength of asphalt concrete offset at low temperature, and they rather deteriorated the strength. Adding CFs was most efficient in enhancing the flexural strength of asphalt concrete compared to other materials (CNT and GNF), which is not consistent with the findings from the indirect tensile strength test results explained above. In contrast to the indirect tensile test, the flexural specimens were subjected to top compressive stress and bottom tensile stress. Since the beams were curved downward due to a bending moment, the flexural crack width was different for different locations along beam height. A larger crack width was obtained at the bottom surface than in parts above it. Therefore, the much longer CFs more effectively bridged the flexural cracks even at larger widths at the bottom than the much shorter CNTs and GNFs, causing higher flexural strengths at both low and ambient temperatures. The improvement of flexural strength of asphalt mixtures by adding carbon fibers (0.75%) was also reported by Wang et al. [34]. We note that the use of CFs is more effective in improving the flexural performance of asphalt concrete than that of CNTs and GNFs, and adding 1.0% CF is recommended to increase the flexural strengths at both ambient and low temperature conditions.

3.6. *Self-healing capability of asphalt concrete with various carbon materials by induction heating*

It is well known that the induction heating method is still very effective for the crack self-healing of asphalt concrete even though the increase in temperature accelerates the aging of asphalt concrete [15,35]. Thus, several previous researchers [10,11,13] have adopted the induction heating method for healing cracks in conductive asphalt concrete. Completely broken specimens under three-point bending were used to examine the effect of carbon material type (i.e., CF, CNT, and GNF) on the self-healing capacity of asphalt concrete by induction heating. The temperature variations of all the broken asphalt concrete specimens with respect to time are shown in Fig. 14. The temperature of plain asphalt concrete without carbon materials did not change with time since they were not conductive. The temperatures of all other asphalt concrete reinforced with CFs, CNTs and GNFs obviously increased with respect to time by induction heating up to 20 min. As shown in Fig. 14, the CF1.0 specimen exhibited the greatest increase in temperature by induction heating, followed by the CNT0.5, GNF0.5, and CF0.5 specimens. Therefore, two important findings were obtained: (1) increasing the amount of CF is beneficial for improving the effectiveness of induction heating of asphalt concrete, and (2) adding CNTs is most effective for improving the induction heating capacity than CF and GNF at an identical content of 0.5%. Very high temperatures, approximately 105 and 120 °C, of asphalt concrete were successfully obtained by a 20-min induction heating process by incorporating 0.5% CFs or GNFs and 0.5% CNTs or 1.0% CFs, respectively. Typical infrared thermographic images of asphalt concrete with 0.5% GNFs with respect to time are summarized in Fig. 15. The maximum temperature (obtained at the center of the specimen where the flexural crack was formed) continuously increased with time during the induction heating process, and the asphalt started to

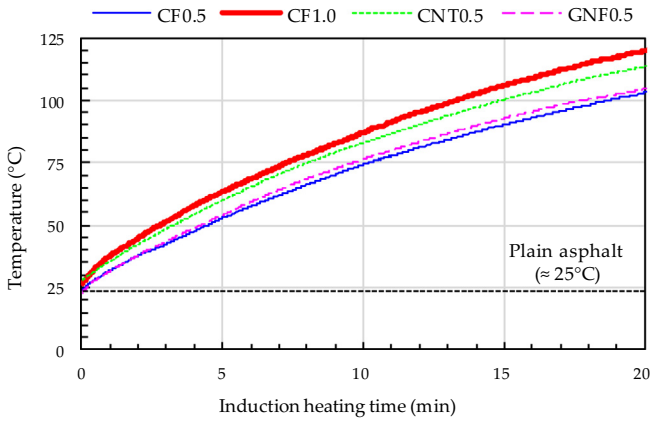

Fig. 14 – Internal temperature versus heating time curves.

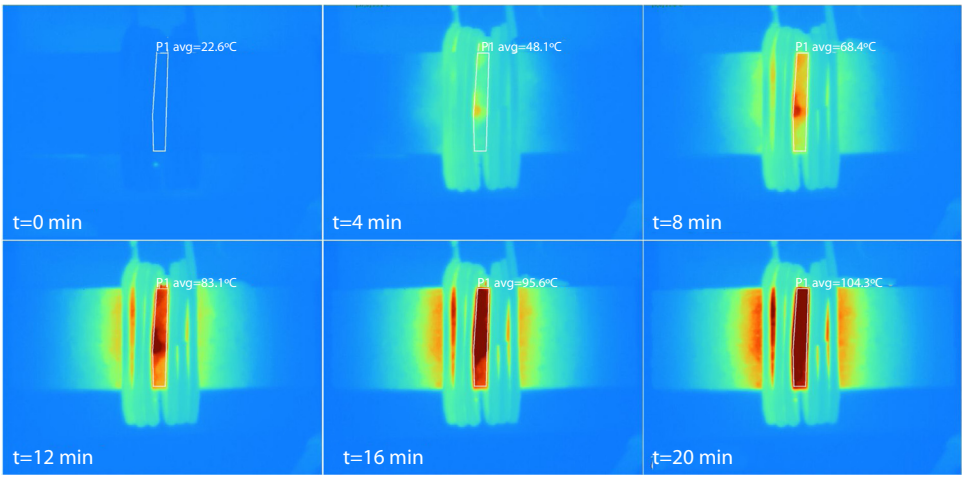

Fig. 15 – Typical infrared thermographic images of asphalt concrete with 0.5% GNFs according to time (Note: t = elapsed time).

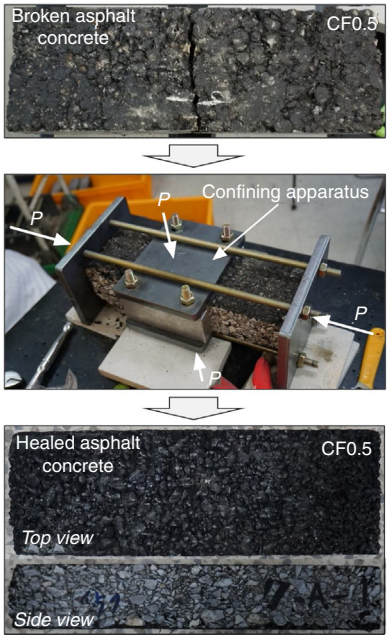

Fig. 16 – Self-healing process of completely broken asphalt concrete.

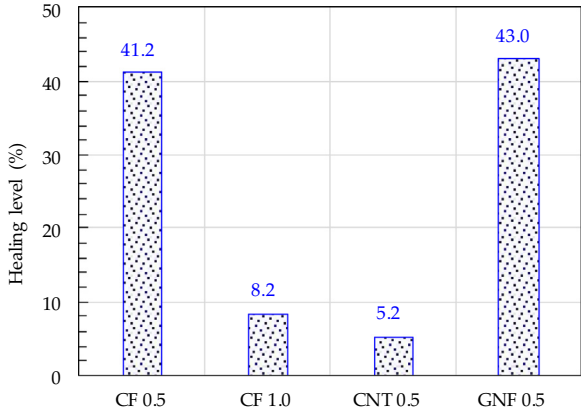

Fig. 17 – Effect of carbon materials on healing level of asphalt concrete.

melt when the maximum temperature was approximately 80 °C.

After reaching the maximum temperature at 20 min, a portion of asphalt at the center of the specimens with CFs, CNTs, and GNFs was melted, and all four surfaces were immediately restrained by steel plates with a thickness of 12 mm and bolts, as shown in Fig. 16, to effectively bond the melted asphalt and to prevent distortion of specimens. Confinement pressure was applied in two directions by tightening the nuts, and they were slowly cooled to ambient temperature for 24 h. Using this process, the completely broken asphalt concrete specimens were healed, as shown in Fig. 16, and the flexural cracks formed by three-point bending tests were not visually observed.

The three-point bending tests of self-healed specimens were carried out again to quantitatively evaluate how much the flexural strength of completely damaged asphalt concrete was recovered by the induction heating process at the ambient temperature. The test setup and apparatus were exactly identical with those used for the undamaged specimens (Fig. 5). The ratio of flexural strengths of self-healed and undamaged virgin specimens was calculated by $f_L = f_{sh}/f_0 \times 100$, and the obtained results are shown in Fig. 17. Herein, f_L is the ratio of flexural strengths of self-healed and virgin specimens, f_{sh} is the flexural strength of self-healed specimens, and f_0 is the flexural strength of virgin specimens. All the damaged asphalt concrete specimens, including the carbon materials, were partially healed by the induction heating process. However, the effectiveness was obviously influenced by the carbon material type. GNF0.5 and CF0.5 specimens exhibited better healing capability than the CF1.0 and CNT0.5 specimens, although their maximum temperature increase observed by induction heating was lower than the latter. For example, the highest value of f_L was found to be 43% for the GNF0.5 specimen, which was about 4%, 422%, and 722% higher than those of CF0.5, CF1.0, and CNT0.5 specimens, respectively. The fluidity of bitumen was greatly increased at a very high temperature of nearly 120 °C, causing separation of a great amount of aggregates

from the bitumen. The broken asphalt concrete specimens were melted and then immediately restrained using a special apparatus (Fig. 16), and they were not compacted. Thus, the highly melted specimens were not effectively healed due to the separation of greater amounts of aggregates, leading to the poorer healing capability, as shown in Fig. 17. Based on this self-healing method using a restraining apparatus, the proper temperature for healing damage to asphalt concrete was around 100 °C, which effectively melted the bitumen and healed the cracks simultaneously. In practice, however, a compacting roller may be more easily applied after melting the damaged asphalt concrete, so that a further study is required to investigate the effects of induction heating and compaction on the self-healing capability of damaged asphalt concrete with carbon materials.

4. Conclusions

In this study, the mechanical and self-healing properties of asphalt concrete with CFs, CNTs, and GNFs were examined. A total of five mechanical tests (Marshall stability, indirect tensile strength, porosity, dynamic stability, and flexural performance) were performed, and an induction heating method was applied to determine the self-healing capability of completely damaged asphalt concrete. Based on the above test results and discussion, the following conclusions are drawn.

Approximately 27% and 12% of the Marshall stability and indirect tensile strength of asphalt concrete were improved by adding 0.5% CNT and GNF, but they were not noticeably influenced by the CFs.

Smaller porosities of asphalt concrete incorporating CNT and GNF were obtained compared to those with and without CFs.

By including 0.5% GNF, about 42% of the dynamic stability of plan asphalt concrete was enhanced and its rate of deformation was also reduced by 40%. The addition of CFs and CNT did not provide any noticeable changes.

Adding CFs was more effective in improving the flexural performance of asphalt concrete than adding CNT and GNF. The use of 1.0% CFs led to about 10% and 50% higher flexural strengths at −10 and 20 °C, respectively, than the plain asphalt concrete and thus is recommended to enhance the flexural performance at both low and ambient temperatures.

Completely failed asphalt concrete was partially self-healed based on carbon materials added and induction heating method. Using 0.5% GNFs and CFs provided the best healing capability of asphalt concrete, leading to about 40% recovery of the original flexural strength.

Conflicts of interest

The author declares no conflicts of interest.

Acknowledgements

This work was supported by the National Research Foundation of Korea (NRF) grant funded by the Korea government (MSIT) (No. 2017R1C1B2007589) and a grant from R&D Program of the Korea Railroad Research Institute, Republic of Korea.

REFERENCES

[1] Faramarzi M, Arabani M, Haghi AK, Motaghitalab V. A study on the effects of CNT's on hot mix asphalt marshal-parameters. In: International Symposium on Advances in Science and Technology. 2011.
[2] Abtahi SM, Sheikhzadeh M, Hejazi SM. Fiber-reinforced asphalt-concrete – a review. Constr Build Mater 2010;24(6):871–7.
[3] Khabiri MM, Alidadi M. Experimental study of the effect of glass and carbon fiber on physical and micro-structure behavior of asphalt. Int J Integr Eng 2017;8(3):1–8.
[4] Latifi H, Hayati P. Evaluating the effects of the wet and simple processes for including carbon nanotube modifier in hot mix asphalt. Constr Build Mater 2018;164:326–36.
[5] Park P, El-Tawil S, Park SY, Naaman AE. Cracking resistance of fiber reinforced asphalt concrete at −20 °C. Constr Build Mater 2015;81:47–57.
[6] Tapkın S. The effect of polypropylene fibers on asphalt performance. Build Environ 2008;43(6):1065–71.
[7] Lee SJ, Rust JP, Hamouda H, Kim YR, Borden RH. Fatigue cracking resistance of fiber-reinforced asphalt concrete. Tex Res J 2005;75(2):123–8.
[8] Selim AA, Taha R, Bayomy F. Laboratory performance of quartzite based stone matrix asphalt mixtures (SMAM). In: Infrastructure: New Materials Methods of Repair A.S.C.E.; 1994. p. 635–42.
[9] Wu SP, Chen Z, Ye QS, Liao WD. Effects of fibre additive on the high temperature property of asphalt binder. J Wuhan Univ Tech-Mater Sci Ed 2006;21(1):118–20.
[10] Yang JM, Kim JK, Yoo DY. Effects of amorphous metallic fibers on the properties of asphalt concrete. Constr Build Mater 2016;128:176–84.
[11] Liu Q, Schlangen E, García Á, van de Ven M. Induction heating of electrically conductive porous asphalt concrete. Constr Build Mater 2010;24(7):1207–13.
[12] Liu Q, Schlangen E, van de Ven M, van Bochove G, van Montfort J. Evaluation of the induction healing effect of porous asphalt concrete through four point bending fatigue test. Constr Build Mater 2012;29:403–9.
[13] García A, Norambuena-Contreras J, Partl MN. Experimental evaluation of dense asphalt concrete properties for induction heating purposes. Constr Build Mater 2013;46:48–54.
[14] Wang Z, Dai Q, Porter D, You Z. Investigation of microwave healing performance of electrically conductive carbon fiber modified asphalt mixture beams. Constr Build Mater 2016;126:1012–9.
[15] Ajam H, Lastra-González P, Gómez-Meijide B, Airey G, Garcia A. Self-healing of dense asphalt concrete by two different approaches: electromagnetic induction and infrared radiation. J Test Eval 2017;45(6):1933–40.
[16] Guideline for the design and construction of asphalt mixtures. Sejong, Korea: Ministry of Land, Infrastructure and Transport; 2014.
[17] Lee SJ, You I, Zi G, Yoo DY. Experimental investigation of the piezoresistive properties of cement composites with hybrid carbon fibers and nanotubes. Sensors 2017;17(11):2516–31.
[18] Yoo DY, You I, Lee SJ. Electrical and piezoresistive sensing capacities of cement paste with multi-walled carbon nanotubes. Arch Civil Mech Eng 2018;18(2):371–84.
[19] Zhang Q, Huang JQ, Zhao MQ, Qian WZ, Wei F. Carbon nanotube mass production: principles and processes. ChemSusChem 2011;4(7):864–89.

[20] Yu MF, Files BS, Arepalli S, Ruoff RS. Tensile loading of ropes of single wall carbon nanotubes and their mechanical properties. Phys Rev Lett 2000;84(24):5552–5.
[21] ASTM D1559. Test method for resistance of plastic flow of bituminous mixtures using Marshall apparatus. Philadelphia, USA: ASTM International; 1989.
[22] Wu S, Ye Q, Li N. Investigation of rheological and fatigue properties of asphalt mixtures containing polyester fibers. Constr Build Mater 2008;22(10):2111–5.
[23] KS 2364. Test method for percent air voids in compacted dense and open bituminous paving mixtures. Seoul, Korea: Korean Agency for Technology and Standard; 2009.
[24] ASTM D6931. Standard test method for indirect tensile (IDT) strength of bituminous mixtures. West Conshohocken, PA: ASTM International; 2012.
[25] KS F2374. Standard test method for wheel tracking of asphalt mixtures. Seoul, Korea: Korean Agency for Technology and Standard; 2010.
[26] KS F2395. Standard test method for bend testing of asphalt mixtures. Seoul, Korea: Korean Agency for Technology and Standard; 2014.
[27] KS 2446. Standard test method of test for bulk specific gravity and density of compacted bituminous mixtures using saturated surface dry specimens. Seoul, Korea: Korean Agency for Technology and Standard; 2000.
[28] KS 2366. Standard test method for theoretical maximum specific gravity of asphalt mixtures. Seoul, Korea: Korean Agency for Technology and Standard; 2010.
[29] Faramarzi M, Arabani M, Haghi AK, Mottaghitalab V. Carbon nanotubes-modified asphalt binder: preparation and characterization. Int J Pavement Res Technol 2015;8(1):29–37.
[30] Ziari H, Farahani H, Goli A, Sadeghpour Galooyak S. The investigation of the impact of carbon nano tube on bitumen and HMA performance. Petroleum Sci Tech 2014;32(17):2102–8.
[31] Amirkhanian AN, Xiao FP, Amirkhanian SN. Characterization of unaged asphalt binder modified with carbon nano particles. Int J Pavement Res Technol 2011;4(5):281–6.
[32] Yang J, Tighe S. A review of advances of nanotechnology in asphalt mixtures. Procedia Soc Behav Sci 2013;96:1269–76.
[33] Qiu K, Chen H, Ye H, Hong J, Sun W, Jiang J. Thermo-mechanical coupling effect on fatigue behavior of cement asphalt mortar. Int J Fatigue 2013;51:116–20.
[34] Wang Z, Gao J, Ai T, Zhao P. Laboratory investigation on microwave deicing function of micro surfacing asphalt mixtures reinforced by carbon fiber. J Testing Eval 2014;42(2):498–507.
[35] Xu S, Tabaković A, Liu X, Schlangen E. Calcium alginate capsules encapsulating rejuvenator as healing system for asphalt mastic. Constr Build Mater 2018;169:379–87.